Direct Geometrico-Static Problem of Underconstrained Cable-Driven Parallel Robots With Three Cables[1]

Marco Carricato
Department of Industrial Engineering
and Interdepartmental Center
for Health Sciences and Technologies,
University of Bologna,
Viale Risorgimento 2,
Bologna, 40136, Italy
e-mail: marco.carricato@unibo.it

This paper studies the direct geometrico-static problem (DGP) of underconstrained cable-driven parallel robots (CDPRs) with three cables. The task consists in determining the end-effector pose and the cable tensile forces when the cable lengths are assigned. The problem is challenging, because kinematics and statics are coupled, and they must be tackled simultaneously. An effective elimination procedure is proposed and a least-degree univariate polynomial free of spurious factors is obtained in the ideal governing the problem. This is proven to admit 156 solutions in the complex field. Several approaches for the efficient computation of the complete solution set are presented, including an eigenproblem formulation and homotopy continuation.
[DOI: 10.1115/1.4024293]

1 Introduction

CDPRs employ cables in place of rigid-body extensible legs in order to control the pose of the end-effector. CDPRs strengthen classic advantages characterizing closed-chain architectures versus serial ones, like reduced moving masses and inertias, a larger payload to robot weight ratio, high dynamic performances, etc., while providing peculiar advantages, such as a larger workspace, reduced manufacturing and maintenance costs, ease of assembly and disassembly, high transportability, and superior modularity and reconfigurability.

It is known that a CDPR intended to control the total number f of degrees of freedom (dofs) of the end-effector, i.e., a *fully constrained* robot, should have at least $f+1$ cables [1]. Indeed, since cables may exert only tensile axial forces, a redundancy of control actions is necessary in order to guarantee that no cable becomes slack [2–5]. However, the number of cables may be reduced if the end-effector is linked to a constraining mechanism [6,7] or it is submitted to an external force of convenient magnitude and direction that steadily acts upon it. One example of the latter case is provided by crane-type manipulators [8,9], in which gravity plays the role of an additional virtual cable. A rich literature exists for fully constrained robots, whose features have been studied under several viewpoints, including workspace analysis [10–17], stiffness [18,19], cable interference [20,21], optimal design [22,23], etc. Conversely, *underconstrained* CDPRs have received little attention in the literature [24–30]. They are equipped with a number of cables n smaller than f, thus allowing only n freedoms of the end-effector to be controlled. The use of CDPRs with a limited number of cables is justified in several applications (such as, for instance, measurement, rescue, service or rehabilitation operations [31–35]), in which the task to be performed requires a limited number of controlled freedoms or a limitation of dexterity is acceptable in order to decrease complexity, cost, set-up time, likelihood of cable interference, etc. Furthermore, a fully constrained CDPR may operate, in appreciable parts of its geometric workspace, as an underconstrained robot, namely, when a full restraint of the end-effector may not be achieved because it would require a negative tension in one or more cables [36–38]. The above considerations motivate a careful study of underconstrained CDPRs.

A major challenge in the kinetostatic analysis of underconstrained CDPRs consists in the intrinsic coupling between kinematics and statics. Indeed, when a fully constrained CDPR operates in the portion of its workspace in which the required set of output wrenches is guaranteed to be applicable with purely tensile cable forces, the pose of the end-effector is determined, in a purely geometrical way, by assigning cable lengths. Conversely, for an underconstrained CDPR, when the actuators are locked and the cable lengths are assigned, the end-effector is still movable, so that the actual configuration is determined by the applied forces. Accordingly, *loop-closure* and *mechanical-equilibrium equations* must be simultaneously solved and displacement analyses become, more properly speaking, *geometrico-static problems* [36,37]. These are significantly more complex than displacement analyses of rigid-link fully constrained manipulators and their solution is a major pending challenge in current kinematics [39].

By taking advantage of the methodology presented in Refs. [36,37], this paper studies the DGP of the 3-3 CDPR, namely, a robot in which a fixed base and a mobile platform are connected to each other by 3 cables (the inverse problem of the 3-3 CDPR is tackled in Ref. [40], whereas the CDPRs suspended by 4 and 5 cables are studied in Refs. [41–43]). The notation 3-3 denotes the number of distinct cable exit points on the base and distinct cable anchor points on the platform. Cables are treated as inextensible and massless, and the platform is acted upon by a constant force, e.g., gravity. The aim of the DGP is to determine the platform pose and the cable tensile forces, when the cable lengths are assigned. This problem is known to be especially difficult [39] and, as yet, only limited results have been presented. Jiang and Kumar [29] reported that the complexity of the involved equations overwhelmed their computer-algebra software. In this paper, successful problem-solving procedures are presented. The following issues, which are classic challenges in robot analysis [44], are specifically dealt with:

(1) determination of the number of solutions in the (zero-dimensional) algebraic variety defined by the problem polynomial equations;
(2) reduction of the problem to a single equation in one unknown (constructive proof of the previous issue);

[1]A preliminary version of this paper was presented at the 2011 IEEE International Conference on Robotics and Automation, Shanghai, China, 2011.

Contributed by the Mechanisms and Robotics Committee of ASME for publication in the Journal of Mechanisms and Robotics. Manuscript received March 24, 2012; final manuscript received April 17, 2013; published online June 24, 2013. Assoc. Editor: Vijay Kumar.

(3) numerical computation of the solution set;
(4) identification of a specific geometry providing the maximal number of distinct real-valued solutions.

With respect to the preliminary conference presentation in Ref. [45], the current version of the paper presents the following enhancements: many algebraic-geometry concepts (concerning Groebner-basis properties, elimination ideals, dialytic elimination, etc.) are presented with more detail, in order to ease reading by a nonspecialized audience; the numerical computation of the solution set is improved, by enhancing the homotopy-continuation algorithms, and by discussing alternative eigenvalue techniques; the problem of the identification of a geometry providing the maximal number of distinct real-valued solutions is addressed. The paper is structured as follows. Section 2 describes the geometrico-static model of the robot. Section 3 presents the problem-solving procedures. Section 4 deals with equilibrium configurations in which some cables may be slack. Section 5 summarizes the main achievements of the paper.

In all numerical examples presented in the text, measurements are expressed in SI units.

2 Geometrico-Static Model

A mobile platform is connected to a fixed base by 3 cables (Fig. 1). The ith cable ($i = 1,\ldots, 3$) exits from the fixed base at point A_i, and it is connected to the mobile platform at point B_i. The cable length is ρ_i, with $\rho_i > 0$. $Oxyz$ is a Cartesian coordinate frame that is fixed to the base, with $\mathbf{i}$, $\mathbf{j}$ and $\mathbf{k}$ being unit vectors along the coordinate axes. $Gx'y'z'$ is a Cartesian frame that is attached to the end-effector. Without loss of generality, O is chosen to coincide with A_1. The platform pose is described by $\mathbf{X} = [\mathbf{x}^T; \mathbf{\Phi}^T]^T$, where $\mathbf{x} = [x, y, z]^T$ is the position vector of G in the fixed frame, and $\mathbf{\Phi}$ is the array grouping the variables parameterizing the platform orientation with respect to $Oxyz$. If Rodrigues parameters [46] are adopted, i.e., $\mathbf{\Phi} = [e_1, e_2, e_3]^T$, the rotation matrix $\mathbf{R}$ between the mobile and the fixed frame is given by

$$\mathbf{R}(\mathbf{\Phi}) = \mathbf{I}_3 + 2\frac{\tilde{\mathbf{\Phi}} + \tilde{\mathbf{\Phi}}\tilde{\mathbf{\Phi}}}{1 + e_1^2 + e_2^2 + e_3^2} \tag{1}$$

where $\tilde{\mathbf{\Phi}}$ denotes the skew-symmetric matrix that is associated with the operator $\mathbf{\Phi}\times$. For the sake of brevity, the following symbols are also introduced:

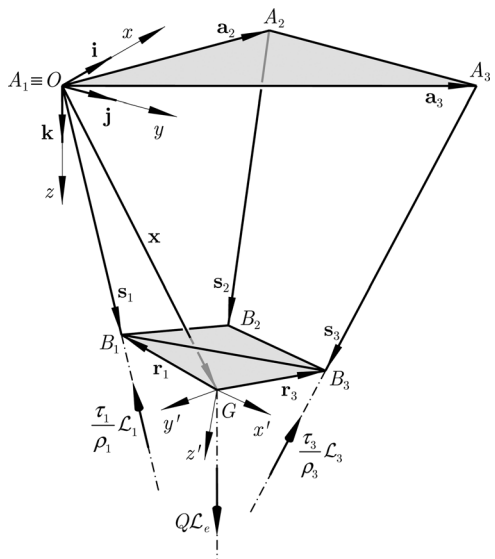

Fig. 1 Model of a cable-driven parallel robot with 3 cables

$$\mathbf{a}_i = A_i - O, \quad \mathbf{r}_i = B_i - G = \mathbf{R}(\mathbf{\Phi})\mathbf{b}'_i,$$
$$\mathbf{s}_i = B_i - A_i = \mathbf{x} + \mathbf{r}_i - \mathbf{a}_i$$

where $\mathbf{b}'_i$ is the position vector of B_i in $Gx'y'z'$. Vector components along the coordinate axes are denoted by right subscripts reporting the axis names.

The platform is acted upon by a constant force, e.g., gravity, which is assumed to be oriented as $\mathbf{k}$ and applied at G, without loss of generality. This force may be described by a zero-pitch wrench $Q\mathcal{L}_e$, where Q is the intensity of the force and $\mathcal{L}_e$ is the normalized Plücker vector of the force line of action. The normalized Plücker vector of the line associated with the ith cable is $\mathcal{L}_i/\rho_i$, where, in axis coordinates, $\mathcal{L}_i = -[\mathbf{s}_i; \mathbf{p}_i \times \mathbf{s}_i]$ and $\mathbf{p}_i$ is any vector from an arbitrarily chosen reference point P (called for brevity *moment pole*) to the cable line. Accordingly, the wrench exerted by the ith cable on the platform is $(\tau_i/\rho_i)\mathcal{L}_i$, with τ_i being a positive scalar representing the intensity of the cable tensile force.

When all cables of the robot are in tension, the set $\mathcal{C}$ of geometrical constraints imposed on the platform comprises three relations in $\mathbf{X}$, i.e.

$$||\mathbf{s}_i||^2 = ||\mathbf{x} + \mathbf{R}(\mathbf{\Phi})\mathbf{b}'_i - \mathbf{a}_i||^2 = \rho_i^2, \quad i = 1, \ldots, 3 \tag{2}$$

By subtracting the first relation from both the second and the third one, and by clearing the denominator $1 + e_1^2 + e_2^2 + e_3^2$, the following equations are obtained:

$$q_1 := H_{200}x^2 + H_{020}y^2 + H_{002}z^2 + H_{100}x + H_{010}y + H_{001}z + H_{000} = 0 \tag{3a}$$
$$q_2 := I_{100}x + I_{010}y + I_{001}z + I_{000} = 0 \tag{3b}$$
$$q_3 := K_{100}x + K_{010}y + K_{001}z + K_{000} = 0 \tag{3c}$$

where all coefficients H_{kmn}, I_{kmn}, and K_{kmn} are quadratic functions of e_1, e_2, and e_3. q_1, q_2, and q_3 have degree 4, 3, and 3 in $\mathbf{X}$, respectively.

As only three geometrical restraints are enforced, the platform preserves three dofs, with its pose being determined by static equilibrium. This may be written as [36,37]

$$\underbrace{[\,\mathcal{L}_1 \quad \mathcal{L}_2 \quad \mathcal{L}_3 \quad \mathcal{L}_e\,]}_{\mathbf{M}} \begin{bmatrix} (\tau_1/\rho_1) \\ (\tau_2/\rho_2) \\ (\tau_3/\rho_3) \\ Q \end{bmatrix} = \mathbf{0} \tag{4}$$

with $\tau_i \geq 0$, $i = 1,\ldots, 3$. After clearing denominators, the polynomials involved in Eq. (4) have degree 3 in $\mathbf{X}$, degree 1 in $\boldsymbol{\tau}$ and total degree 4 in $\mathbf{Y}$, where $\boldsymbol{\tau} = [\tau_1, \tau_2, \tau_3]^T$ and $\mathbf{Y} = [\mathbf{X}^T, \boldsymbol{\tau}^T]^T$.

When solving the DGP, cable lengths are assigned. Accordingly, Eqs. (3) and (4) form a system S of nine polynomial relations comprising nine variables, i.e., $\mathbf{X}$ and $\boldsymbol{\tau}$. These relations are coupled, and they must be solved simultaneously. By counting solutions at infinity, the number of isolated roots (including multiplicities) is equal to the minimal multihomogeneous Bezout number of S [47,48]. This number is usually an indicator of the complexity of the problem to be solved. By searching all possible multihomogenizations of S [49], the minimal Bezout number emerges by partitioning $\mathbf{Y}$ as $[\{x, y, z\}, \{e_1, e_2, e_3\}, \{\tau_1, \tau_2, \tau_3\}]$, and it is equal to 4800. This number is very high.

Following [36,37], the problem may be simplified by eliminating cable tensions from the set of unknowns. Indeed, Eq. (4) holds only if

$$\text{rank}(\mathbf{M}) \leq 3 \tag{5}$$

namely, if $\mathcal{L}_1, \mathcal{L}_2, \mathcal{L}_3$, and $\mathcal{L}_e$ are linearly dependent. This is a purely geometrical condition, since $\mathbf{M}$ is a 6×4 matrix that only

depends on the platform pose. By setting all 4×4 minors of $\mathbf{M}$ equal to zero, a set of 15 scalar relations that do *not* contain cable tensions may be obtained.[2]

If O is chosen as the moment pole, $\mathcal{L}_i$ and $\mathcal{L}_e$ may be respectively expressed, in axis coordinates, as $-[\mathbf{s}_i; \mathbf{a}_i \times \mathbf{s}_i]$ and $[\mathbf{k}; \mathbf{x} \times \mathbf{k}]$, so that $\mathbf{M}$ becomes

$$\mathbf{M}(O) = \begin{bmatrix} -\mathbf{s}_1 & -\mathbf{s}_2 & -\mathbf{s}_3 & \mathbf{k} \\ \mathbf{0} & -\mathbf{a}_2 \times \mathbf{s}_2 & -\mathbf{a}_3 \times \mathbf{s}_3 & \mathbf{x} \times \mathbf{k} \end{bmatrix} \tag{6}$$

The equations[3]

$$p_1 := \det \mathbf{M}_{1236}(O) = 0 \tag{7a}$$

$$p_2 := \det \mathbf{M}_{1235}(O) = 0 \tag{7b}$$

$$p_3 := \det \mathbf{M}_{1234}(O) = 0 \tag{7c}$$

comprise the lowest-degree polynomials in $\mathbf{X}$ among all minors of $\mathbf{M}(O)$. They are of degree 4 in $\mathbf{\Phi}$ and degree 2 in $\mathbf{x}$, thus being of total degree 6 in $\mathbf{X}$. All other minors have degree ranging from 7 to 9 in $\mathbf{X}$.

An additional sextic relation in $\mathbf{X}$ emerges by setting $\det \mathbf{M}_{j456}(O) = 0$ for $j = 1,\ldots, 3$, so that

$$\mathbf{s}_1 \left[\det \mathbf{M}_{456,234}(O)\right] = \mathbf{0} \tag{8}$$

and thus, since $\mathbf{s}_1 \neq 0$ when $\rho_1 > 0$

$$p_4 := \det \mathbf{M}_{456,234}(O) = 0 \tag{9}$$

Equation (9) is, indeed, of degree 4 in $\mathbf{\Phi}$, degree 2 in $\mathbf{x}$ and, thus, total degree 6 in $\mathbf{X}$. Additional linearly independent sextic equations in $\mathbf{X}$ may be derived as follows.

Let $\mathbf{M}$ be written by choosing a generic point P as the moment pole, i.e.

$$\mathbf{M}(P) = \begin{bmatrix} \cdots & -\mathbf{s}_i & \cdots & \mathbf{k} \\ \cdots & -(B_i - P) \times \mathbf{s}_i & \cdots & (G - P) \times \mathbf{k} \end{bmatrix} \tag{10}$$

When $P \equiv B_i$ and $P \equiv A_i$, $i = 1,\ldots, 3$, the moment vector in the ith column vanishes, so that setting $\det \mathbf{M}_{j456}(B_i) = 0$ and $\det \mathbf{M}_{j456}(A_i) = 0$ for $j = 1,\ldots, 3$ yields, respectively

$$\mathbf{s}_i \left[\det \mathbf{M}_{456,km4}(B_i)\right] = \mathbf{0} \tag{11}$$

and

$$\mathbf{s}_i \left[\det \mathbf{M}_{456,km4}(A_i)\right] = \mathbf{0} \tag{12}$$

with $k, m \in \{1, 2, 3\} - \{i\}$. Since $\mathbf{s}_i \neq 0$ for any i, the following equations

$$p_5 := \det \mathbf{M}_{456,234}(B_1) = 0 \tag{13a}$$

$$p_6 := \det \mathbf{M}_{456,134}(B_2) = 0 \tag{13b}$$

$$p_7 := \det \mathbf{M}_{456,134}(A_2) = 0 \tag{13c}$$

$$p_8 := \det \mathbf{M}_{456,124}(B_3) = 0 \tag{13d}$$

$$p_9 := \det \mathbf{M}_{456,124}(A_3) = 0 \tag{13e}$$

are accordingly obtained.

Analogously, by defining an additional convenient point G_0 such that $G - G_0 = \mathbf{k}$, and by setting $P \equiv G$ and $P \equiv G_0$, one also obtains

$$p_{10} := \det \mathbf{M}_{456,123}(G) = 0 \tag{14a}$$

$$p_{11} := \det \mathbf{M}_{456,123}(G_0) = 0 \tag{14b}$$

All polynomials p_j, $j = 5,\ldots, 11$, have degree 4 in $\mathbf{\Phi}$, degree 2 in $\mathbf{x}$, and total degree 6 in $\mathbf{X}$. No other linearly independent sextic in $\mathbf{X}$ may be obtained from the minors of $\mathbf{M}$ by varying the moment pole. Polynomials $p_1,\ldots, p_{11}$ (which contain six variables) are *linearly independent*, but still *dependent* in a *nonlinear* way.

3 Problem-Solving Algorithms

Solving the DGP of the 3-3 CDPR requires solving, simultaneously, both the equations emerging from the geometrical constraints and those inferred from static equilibrium. The point-to-point distance relations in Eq. (3) represent the typical constraints governing the forward kinematics of parallel manipulators equipped with telescopic legs connected to the base and the platform by ball-and-socket joints. In particular, the DGP of the general Gough-Stewart manipulator depends on six equations of this sort, one of which is equivalent to Eq. (3*a*) and five more to Eqs. (3*b*) and (3*c*). This problem is known to be very difficult and it has attracted the interest of researchers for several years [50]. The DGP of the 3-3 CDPR appears to be an even more complex task, since, in this case, three equations analogous to Eqs. (3*b*) and (3*c*), namely of degree 3 in $\mathbf{X}$, are replaced by relationships that are, at least, of degree 6 in $\mathbf{X}$.

In the following, the four challenges mentioned at the end of the Introduction are taken on.

3.1 Number of Solutions in the Complex Field. Let $\langle J \rangle$ be the ideal generated by the set of polynomials $J = \{q_1, q_2, q_3, p_1, \ldots, p_{11}\}$. q_1, q_2, and q_3 have, respectively, degree 4, 3, and 3 in $\mathbf{X}$, whereas all other generators in J have degree 6 in $\mathbf{X}$. For a generic choice of the robot geometric parameters, J contains 348 monomials in $\mathbf{X}$. In order to ease numeric computation via a computer-algebra system, namely, the *Groebner Package* provided within the mathematical software *Maple*, all geometric parameters are assigned generic *rational values*. Accordingly, $\langle J \rangle \subset \mathbb{Q}[\mathbf{X}]$, where $\mathbb{Q}[\mathbf{X}]$ is the set of all polynomials in $\mathbf{X}$ with coefficients in $\mathbb{Q}$. In the following, all Groebner bases are assumed to be reduced and they are computed with respect to *graded reverse lexicographic monomial order* (grevlex, in brief). The lexicographic monomial order is particularly suitable to solve systems of polynomial equations, for it provides polynomial sets whose variables may be eliminated successively. However, the Groebner bases that it provides tend to be very large and thus, even for problems of moderate complexity, they have little chance to be actually computable. Conversely, the graded reverse lexicographic order produces bases that are endowed with no particular structure suitable for elimination purposes, but it provides for more efficient calculations.

In general, a Groebner basis $G[J]$ of $\langle J \rangle$ with respect to grevlex($\mathbf{X}$), with variables ordered so that $z > y > x > e_1 > e_2 > e_3$, may be computed in a fairly expedited way. A key factor for the efficiency of such a computation is the *abundance of generators* available in J, which greatly simplifies and speeds up calculation (a feature already pointed out in Ref. [51]). For instance, by exploiting all 14 generators in J, the computation of $G[J]$ for the exemplifying 3-3 CDPR whose dimensions are reported in Table 2 requires roughly 1.3 min on a PC with a 2.67 GHz Intel Xeon processor and 4 GB of RAM. If only six generators are used, computation time is 30 times higher and, most important, spurious solutions are introduced in the solution set (Eq. (5) requires *all* minors of $\mathbf{M}$ to be zero).

[2] In very special cases, it may happen that Eq. (5) is fulfilled because $\mathcal{L}_1$, $\mathcal{L}_2$ and $\mathcal{L}_3$ become linearly dependent. In these configurations, equilibrium is not possible if $\text{rank}(\mathbf{M}) = 3$, since the external wrench would not belong to the screw subspace generated by the cable lines. Configurations like these need to be discarded from the solution set.

[3] The notation $\mathbf{M}_{hij,klm}$ denotes the block matrix obtained from rows h, i and j, and columns k, l and m, of $\mathbf{M}$. When all columns of $\mathbf{M}$ are used, the corresponding subscripts are omitted.

Once $G[J]$ is known, the normal set $\mathbf{N}[J]$ of $\langle J\rangle$, i.e., the set of all monomials that are *not* multiples of any leading monomial in $G[J]$, may be easily computed. In this case, $\mathbf{N}[J]$ is (in vector format)

$$\mathbf{N}[J] = \left[1, e_1, e_2, e_3, x, y, z, e_1^2, e_1e_3, \ldots, xze_1e_2\right]^T \tag{15}$$

and it comprises 156 monomials. For the properties of Groebner bases, the number of monomials in $\mathbf{N}[J]$ coincides with the number of complex roots in the algebraic variety V of $\langle J\rangle$, including multiplicities, namely with the number of solutions of the problem at hand [52].

3.2 Least-Degree Univariate Polynomial. This Section aims at computing a least-degree univariate polynomial in $\langle J\rangle$. Some methods that are available in the literature are reviewed and a novel technique is presented.

3.2.1 The Elimination-Ideal Approach. In order to eliminate unknowns and solve J, Groebner bases with respect to some elimination monomial orders are needed. If $\mathbf{X}_l$ is a list of l variables in $\mathbf{X}$ and $\mathbf{X}\backslash\mathbf{X}_l$ is the (ordered) relative complement of $\mathbf{X}_l$ in $\mathbf{X}$, the lth elimination ideal $\langle J_l\rangle$ of $\langle J\rangle$ is defined as $\langle J\rangle \cap \mathbb{Q}[\mathbf{X}\backslash\mathbf{X}_l]$, namely as the subset of all polynomials of $\langle J\rangle$ that comprise variables in $\mathbf{X}\backslash\mathbf{X}_l$ only (and in which, thus, the l variables in $\mathbf{X}_l$ have been eliminated). As $\langle J\rangle$ comprises six unknowns, the polynomials of $\langle J_1\rangle$ contain only five variables, the polynomials of $\langle J_2\rangle$ only four, and so on. $\langle J_5\rangle$ comprises a single variable and, thus, it contains the least-degree polynomial of $\langle J\rangle$ in that variable. A monomial order $>_l$ on $\mathbb{Q}[\mathbf{X}]$ is of l-elimination type provided that any monomial involving a variable in $\mathbf{X}_l$ is greater than any monomial in $\mathbb{Q}[\mathbf{X}\backslash\mathbf{X}_l]$. It may be proven that, if $G_{>l}[J]$ is a Groebner basis of $\langle J\rangle$ with respect to $>_l$, then $G_{>l}[J] \cap \mathbb{Q}[\mathbf{X}\backslash\mathbf{X}_l]$ is a basis of the lth elimination ideal $\langle J_l\rangle$ [53]. The l-elimination monomial order implemented in *Maple* is a product order that induces grevlex orders on both $\mathbb{Q}[\mathbf{X}_l]$ and $\mathbb{Q}[\mathbf{X}\backslash\mathbf{X}_l]$.

In this perspective, the FGLM algorithm [54], which converts a Groebner basis from one monomial order to another, may be called upon to derive $G_{>l}[J]$ from $G[J]$. Once $G_{>l}[J]$ is known, one may extract the subset $G[J_l]$ of all polynomials of $G_{>l}[J]$ that comprise variables in $\mathbf{X}\backslash\mathbf{X}_l$ only. For the aforementioned property, $G[J_l]$ is a Groebner basis of $\langle J_l\rangle$ with respect to grevlex$(\mathbf{X}\backslash\mathbf{X}_l)$. The structure of $G[J_l]$, as obtained by the FGLM algorithm, is illustrated in Table 1 for $l = 0,\ldots, 5$. This structure holds for any *generic* choice of the robot parameters. Column 2 specifies the variables appearing in $\langle J_l\rangle$. Column 3 reports the number N_l of generators in $G[J_l]$. Column 4 provides the degree in $\mathbf{X}\backslash\mathbf{X}_l$ of such generators (in parentheses, the number of generators having a certain degree is specified). Columns 5 and 6 report, for each variable $w \in \mathbf{X}\backslash\mathbf{X}_l$, the highest power of w in $G[J_l]$ and the number of monomials in $G[J_l]$ having variables in $\mathbf{X}\backslash\mathbf{X}_l - \{w\}$, respectively. Since the presented elimination ideals are based on the sequential elimination of variables z, y, x, e_1, and e_2, $G[J_5]$ coincides (up to a scalar multiple) with the least-degree polynomial of $\langle J\rangle$ in e_3. This polynomial has degree 156. Clearly, if a different elimination sequence is chosen, a different structure is obtained, and a 156th-degree univariate polynomial in another unknown may be achieved.

In theory, by computing elimination ideals via the FGLM algorithm, a least-degree polynomial in one variable may be calculated. In practical cases, however, the procedure may likely fail, due to an excessively onerous computational burden. Section 3.2.3 will show that computing $\langle J_l\rangle$ is very demanding in terms of both computation time and memory usage. Performing the elimination of the "last" variables, in particular, is extremely onerous and it is likely to prove unfeasible on normal workstations.

3.2.2 Sylvester's Dialytic Approach. Another strategy to compute a univariate polynomial in $\langle J\rangle$ consists in deriving a Sylvester-type eliminant matrix [44]. A crucial step in doing so consists in finding, by either heuristic or algorithmic methods, viable ways to augment the original set of equations to obtain a square homogeneous linear system, without introducing spurious solutions. The larger the final system is, the heavier the computational burden required by the resultant expansion proves to be and the likelier extraneous polynomial factors are to appear. Heuristic methods usually provide smaller eliminant matrices, but they rely on procedures specifically tailored for the ideals at hand and they are very difficult to conceive for high-degree problems, characterized by a large gap between the original number of equations and the number of monomials therein involved. Conversely, algorithmic approaches are based on procedures guaranteed to deliver a set of polynomials having the necessary properties to form an eliminant, even though this may not have the least size. Since J comprises 14 polynomials and 348 monomials, algorithmic methods are preferred here. In this context, two main procedures are available in the literature, both exploiting a prior knowledge of the Groebner basis $G[J]$.

One procedure is based on the properties of Groebner bases and normal sets [55,56]. Let the polynomial $w\eta_h$ be considered, with $w \in \mathbf{X}$ and with η_h being the hth monomial in $\mathbf{N}[J]$. If r_h is the remainder on division of $w\eta_h$ by $G[J]$, r_h is a linear combination of monomials in $\mathbf{N}[J]$, i.e., $r_h = \sum_{k=1}^{156} a_{hk}\eta_k$, with a_{hk} being a constant coefficient. Since $r_h - w\eta_h$ belongs to $\langle J\rangle$, it must vanish on V. By assembling all the equations that may be obtained this way for $h = 1,\ldots, 156$, one has

$$(\mathbf{A}[J, w] - w\mathbf{I}_{156})\mathbf{N}[J] = \mathbf{0} \tag{16}$$

where $\mathbf{A}[J, w] = [a_{hk}]$ is a 156×156 numeric matrix (called *multiplication matrix* for w) and $\mathbf{I}_{156}$ is the 156×156 identity matrix. Equation (16) is a linear eigenvalue problem, whose 156th-degree characteristic polynomial is the desired resultant in w. While the formulation (16) provides an efficient way to compute all 156 solutions of the problem by numerical means (see Sec. 3.3), it is not likewise effectual for the computation of the resultant, since it requires the expansion of a 156×156 matrix, which is a very demanding computational operation.

Another method to compute a least-degree univariate polynomial from $G[J]$ is presented in Refs. [51]. It is based on the identification of a subset $H[J]$ of $G[J]$ and a variable $w \in \mathbf{X}$ such that the number of generators in $H[J]$ equals the number of monomials in the variables of $\mathbf{X} - \{w\}$ appearing in the polynomials of $H[J]$.

Table 1 Structure of the Groebner bases of the elimination ideals $\langle J_l\rangle$ of $\langle J\rangle$ for any 3-3 CDPR of generic geometry

$G[J_l]$	$\mathbf{X}\backslash\mathbf{X}_l$	N_l	Degrees of the generators in $\mathbf{X}\backslash\mathbf{X}_l$	Highest degree in w, $w \in \mathbf{X}\backslash\mathbf{X}_l$	No. of monomials with variables in $\mathbf{X}\backslash\mathbf{X}_l - \{w\}$, $w \in \mathbf{X}\backslash\mathbf{X}_l$
$G[J]$	$[z, y, x, e_1, e_2, e_3]$	137	3(2), 4(41), 5(94)	4, 4, 4, 4, 5, 5	183, 183, 172, 181, 150, 137
$G[J_1]$	$[y, x, e_1, e_2, e_3]$	126	5(96), 6(30)	5, 5, 5, 5, 6	145, 144, 142, 141, 126
$G[J_2]$	$[x, e_1, e_2, e_3]$	84	6(54), 7(30)	6, 6, 6, 7	98, 98, 94, 84
$G[J_3]$	$[e_1, e_2, e_3]$	45	8(9), 9(36)	8, 8, 9	53, 53, 45
$G[J_4]$	$[e_2, e_3]$	18	17(15), 18(3)	17, 18	19, 18
$G[J_5]$	$[e_3]$	1	156(1)	156	—

This way, $H[J]$ (possibly coinciding with $G[J]$) may be set up as a square system of homogeneous linear equations in the monomials of $\mathbf{X}-\{w\}$, whose coefficients only depend on w. An eliminant matrix may be thus constructed and a resultant in w computed. For the problem at hand, $G[J]$ comprises 137 generators. By choosing $w \neq e_3$, the number of monomials in $\mathbf{X}-\{w\}$ proves to be greater than 137, but, by choosing $w = e_3$ (e_3 is the "smallest" variable in the monomial ordering chosen to compute $G[J]$) the number of monomials in $\mathbf{X}-\{e_3\}$ is exactly equal to 137 (see Table 1). By this approach, the resultant in w emerges from the expansion of a 137×137 matrix, which is still a very expensive computational task.

3.2.3 A Novel Hybrid Approach. The approach followed in this paper is a hybrid variant of those previously described. It emerges from the observation that the method proposed by Dhingra et al. [51] may be applied to the Groebner basis of any elimination ideal of $\langle J\rangle$, since Table 1 shows that, if e_3 is the smallest variable in $\mathbf{X}\backslash\mathbf{X}_l$, $G[J_l]$ comprises a number of monomials in $\mathbf{X}\backslash\mathbf{X}_l-\{e_3\}$ that is equal to N_l for all values of l. For example, the Groebner basis $G[J_3]$ of $\langle J\rangle \cap \mathbb{Q}[e_1,e_2,e_3]$ with respect to grevlex(e_1,e_2,e_3) comprises 45 polynomials (9 of degree 8 in $\mathbf{\Phi}$ and 36 of degree 9 in $\mathbf{\Phi}$), including 45 monomials in e_1 and e_2 (of degree ranging from 0 to 8).

It follows that, if e_3 is assigned the role of "hidden" variable, the generators of $G[J_l]$ may be written, for any l, in the form

$$\mathbf{D}_l\mathbf{E}_l = \left(\sum_{k=0}^{u} e_3^k \mathbf{B}_{l,k}\right)\mathbf{E}_l = \mathbf{0} \tag{17}$$

where u is the highest power of e_3 in $G[J_l]$, $\mathbf{B}_{l,k}$ is a $N_l \times N_l$ numeric matrix, $\mathbf{D}_l$ is a matrix polynomial of degree u in e_3, and $\mathbf{E}_l$ is a N_l-dimensional vector comprising all monomials in $G[J_l]$ having variables in $\mathbf{X}\backslash\mathbf{X}_l-\{e_3\}$. Accordingly, the desired resultant, free from extraneous polynomial factors, is

$$G[J_5] = \det \mathbf{D}_l = \sum_{h=0}^{156} L_h e_3^h = 0 \tag{18}$$

where coefficients L_h only depend on the robot geometric parameters.

The advantage gained by applying a dialytic step to a Groebner basis $G[J_l]$ with $l > 0$ results from the data presented in Table 2. This table reports, for an exemplifying robot, the CPU time required to compute grevlex bases for the elimination ideals of $\langle J\rangle$, with $l = 0,\ldots, 5$, on the PC mentioned in Sec. 3.1. In particular, the third column reports the CPU time $T_{G[J_l]}$ required to obtain $G[J_l]$ by computing $\langle J\rangle \cap \mathbb{Q}[\mathbf{X}\backslash\mathbf{X}_l]$ or, in parentheses, $\langle J_{l-1}\rangle \cap \mathbb{Q}[\mathbf{X}\backslash\mathbf{X}_l]$, by the FGLM algorithm. As remarked in Sec. 3.2.1, the elimination task proves to be computationally very expensive and time consuming. In particular, the "deeper" the elimination process (i.e., the smaller the number of variables in $\mathbf{X}\backslash\mathbf{X}_l$), the longer the time necessary to perform the computation and, mainly, the larger the amount of memory that is required. The latter issue is particularly critical. Indeed, for the example at hand, the last elimination ideal cannot be computed on the given PC, due to excessive memory usage.[4]

The fourth column of Table 2 reports the CPU time $T_{G[J_5]}$ required to calculate $G[J_5]$ by applying Sylvester's dialytic elimination to $G[J_l]$, for $l = 0,\ldots, 4$. In this case, computation time depends on the dimension of $\mathbf{D}_l$ and, thus, it normally decreases with the number of variables in $\mathbf{X}\backslash\mathbf{X}_l$. Memory requirements are modest and the algorithm is ordinarily successful. The fastest computation is obtained by computing $\langle J_3\rangle$ via the FGLM algorithm, thus eliminating $\{x, y, z\}$, and then applying dialytic elimination to $G[J_3]$, thus eliminating $\{e_1, e_2\}$. The former step requires 49 min, whereas the latter 33 min. The overall computation time (including the time necessary to calculate $G[J]$) is $1.3 + 49 + 33 \approx 83$min. By considering the size of $G[J_5]$, calculation proves to be particularly efficient, thus requiring less than 1/20 of the time that would be necessary by applying dialytic elimination directly to $G[J]$ (i.e., roughly 1919 min), as proposed in Ref. [51]. Due to space limitations, the expression of $G[J_5]$ for the example at hand is not explicitly reported.

Table 2 Computation time to obtain Groebner bases of the elimination ideals $\langle J_l\rangle$ for a robot with $\mathbf{a_2} = [\mathbf{10}; \mathbf{0}; \mathbf{0}]$, $\mathbf{a_3} = [\mathbf{0}; \mathbf{12}; \mathbf{0}]$, $\mathbf{b'_1} = [\mathbf{1}; \mathbf{0}; \mathbf{0}]$, $\mathbf{b'_2} = [\mathbf{0}; \mathbf{1}; \mathbf{0}]$, $\mathbf{b'_3} = [\mathbf{0}; \mathbf{0}; \mathbf{1}]$, and $(\boldsymbol{\rho}_1, \boldsymbol{\rho}_2, \boldsymbol{\rho}_3) = (\mathbf{7.5}, \mathbf{10}, \mathbf{9.5})$

l	$\langle J_l\rangle$	$T_{G[J_l]}$ (min)	$T_{G[J_5]}$ (min)
0	$\langle J\rangle$	1.3	1919
1	$\langle J\rangle \cap \mathbb{Q}[y, x, e_1, e_2, e_3]$	19	2159
2	$\langle J\rangle \cap \mathbb{Q}[x, e_1, e_2, e_3]$	42 (27)	579
3	$\langle J\rangle \cap \mathbb{Q}[e_1, e_2, e_3]$	49 (24)	33
4	$\langle J\rangle \cap \mathbb{Q}[e_2, e_3]$	160 (80)	11
5	$\langle J\rangle \cap \mathbb{Q}[e_3]$	…	–

The hybrid elimination procedure described here was tested on several robot geometries. Throughout the numerical experimentation, the fastest computation of $G[J_5]$ was always obtained by first computing $\langle J_3\rangle$ and then applying dialytic elimination to $G[J_3]$. On this basis, a simple automation of the presented elimination algorithm may be implemented, including a stage that eliminates $\{x, y, z\}$ by the FGLM algorithm and a subsequent dialytic step that eliminates $\{e_1, e_2\}$. It is noteworthy that the partition $[\{x, y, z\}, \{e_1, e_2, e_3\}]$ of $\mathbf{X}$ leads to the minimal multihomogeneous Bezout number of the generators of $\langle J\rangle$ (see Sec. 3.3.2). This observation may suggest an algorithmic heuristic to determine a priori which variables may be most conveniently eliminated by the FGLM procedure before attempting the dialytic step.

It emerges from the above considerations that the presented hybrid approach provides a profitable strategy to compute a least-degree univariate polynomial in $\langle J\rangle$, which may succeed when other methods (such as those derived from Refs. [51,54–56]) either fail or prove to be too onerous in terms of computational burden. The bottleneck of the procedure is the strong dependence of the computation performance on the "size" of the coefficients expressing the robot geometric parameters. Indeed, the latter must be assigned *rational* values, which are ordinarily obtained by converting real values. The higher the number of digits in the original floating-point data, the bigger the numerators and denominators of the resulting rationals, and the larger the size of the coefficients in the polynomials forming the ideal. As a result, computation becomes much slower and memory-demanding. This is a limitation shared by all computational methods based on Groebner bases.

3.3 Numerical Computation of the Solution Set. For the numeric solutions of the problem to be actually calculated, working with a polynomial of degree 156 is unpractical and it poses substantial numerical problems. In this perspective, several alternative options are considered.

3.3.1 Eigenvalue Formulations. An efficient technique, which eliminates the burdensome operations related to the expansion of the determinant in Eq. (18), consists in setting up Eq. (17) as a polynomial eigenvalue problem [57]. The roots of Eq. (18) and the corresponding vectors $\mathbf{E}_l$ (from which the solutions in $\mathbf{X}\backslash\mathbf{X}_l-\{e_3\}$ may be immediately obtained) are, respectively, the eigenvalues and eigenvectors of $\mathbf{D}_l$. The most widely used approach to compute these eigenpairs is the conversion of Eq. (17) into a linear eigenproblem of order uN_l with the same finite eigenvalues, so that classical methods for generalized eigenproblems may be pressed into service.

[4]In a computation performed on a more powerful workstation, *Maple* estimated a memory usage of about 12GB, in order to derive $\langle J_5\rangle$ from $\langle J_4\rangle$.

For the robot whose dimensions are reported in Table 2, the command *Polyeig* available within the mathematical software *Matlab* computes (on the PC mentioned in Sec. 3.1) all eigenpairs of $\mathbf{D}_0$ (which is the matrix polynomial obtained from $G[J]$) in roughly 1 s. Accuracy is good, provided that $\mathbf{D}_0$ is conditioned by premultiplying it by $\mathbf{B}_{0,0}^{-1}$ [58,59].

An even faster computation is provided by the linear formulation presented in Eq. (16). In this case, the 156 eigenpairs of $\mathbf{A}[J, e_3]$ are accurately computed by the *Matlab* command *Eig* in roughly 0.03 s. Since the first seven entries of $\mathbf{N}[J]$ are $1, e_1, e_2, e_3, x, y, z$ (see Eq. (15)), a unique solution in $\mathbf{X}$ emerges from each eigenvector in a straightforward manner.

A drawback of the eigen approaches described above is that both of them require a prior computation of $G[J]$. As observed at the end of Sec. 3.2.3, the efficiency of the computation of a Groebner basis highly depends on the size of the rational coefficients of the polynomials generating the basis. For the robot in Table 2, $G[J]$ may be computed in as low as 1.3 min, because the rationals representing the robot parameters may be expressed via one- or two-digit integers. Instead, for the robot whose dimensions are reported in the subsequent Table 4, the conversion of real parameters into rationals brings in six-digit integer denominators and numerators, and the computation of $G[J]$ requires more than 1 h.

Once an equilibrium configuration $\mathbf{X}$ is found, it proves *feasible* only if it is *stable* and therein cable tensions are *positive*. Cable tensions may be obtained by any three suitable relations chosen within Eq. (4), e.g., if $\mathbf{s}_1, \mathbf{s}_2$, and $\mathbf{s}_3$ are linearly independent, as

$$\begin{bmatrix} \tau_1 \\ \tau_2 \\ \tau_3 \end{bmatrix} = -\left[\frac{\mathbf{s}_1}{\rho_1}\frac{\mathbf{s}_2}{\rho_2}\frac{\mathbf{s}_3}{\rho_3}\right]^{-1} Q\mathbf{k} \tag{19}$$

Stability may be assessed by the definiteness of the reduced Hessian $\mathbf{H}_r$, as explained in Ref. [37]. Due to space limitations, Table 3 reports only the *real* solutions of the DGP of the robot presented in Table 2. The symbols $>, \geq, <, \leq$ and $<>$ denote, respectively, a positive-definite, a positive-semidefinite, a negative-definite, a negative-semidefinite and an indefinite Hessian matrix. In this case, 10 out of 156 solutions are real and, among them, only 6 have nonnegative tension in all cables. These are shown in Fig. 2. Only the configuration in Fig. 2(*b*) is stable and, thus, feasible.

3.3.2 Homotopy Continuation. An alternative approach with respect to the eigenvalue formulations presented in Sec. 3.3.1 is offered by homotopy continuation [52]. Continuation has the significant advantage that it requires no prior Groebner-basis computation by a computer-algebra system and real-value geometric parameters may be directly handled in floating-point arithmetic. Accordingly, the dependence of computation time on the specific values of the robot parameters is rather modest.

If no information is a priori known about the roots in the variety V of J, the DGP of the 3-3 CDPR may be cast, on the basis of the degree of the polynomials contained in J, into the larger family of all polynomial systems made up by one quartic, two cubics and three sextics on $\mathbf{X} \in \mathbb{P}^6$. By counting solutions at infinity, a general member of this family, e.g., $J_{\text{red}} = \{q_1, q_2, q_3, p_1, p_2, p_3\}$, has a number of isolated roots equal to the minimal multihomogeneous Bezout number [47,48]. This is also the number of paths tracked by the homotopy-continuation software used in this paper, i.e., BERTINI [60]. By searching all possible multihomogenizations [49], the minimal Bezout number of J_{red} emerges when $\mathbf{X}$ is partitioned as $[\{x, y, z\}, \{e_1, e_2, e_3\}]$ and it is equal to 1920. Computation converges in a robust way. For the robot in Table 2, BERTINI computes finite solutions to J_{red} in roughly 10 min (on the same PC mentioned earlier and by adopting BERTINI default settings). However, since only three relations (i.e., p_1, p_2, and p_3) are used within those that emerge from Eq. (5) to form, together with Eq. (3), a square system of six equations in six unknowns (and, thus, only three minors of $\mathbf{M}$ are set to zero), spurious solutions, for which some of the unused minors of $\mathbf{M}$ do not vanish, are introduced. Therefore, the roots computed by BERTINI must be sifted in order to retain only those that actually lie in V. As expected, 156 solutions are finally obtained.

The above procedure is suitable to solve the DGP of the 3-3 robot under the assumption that no information is known about the number of roots in $\mathbb{C}^6$. Once the latter information is known, a more efficient continuation technique may be used to numerically solve practical cases. Indeed, the complete family of the DGPs of 3-3 CDPRs lies in a 21-dimensional parameter space, parametrized by the geometric quantities $\mathbf{a}_i, \mathbf{b}'_i$ and ρ_i, $i = 1,\ldots, 3$. Accordingly, when the 156 isolated roots of the DGP are known for a generic "start" robot geometry, *parameter* homotopy continuation may be used to find solutions for any other "target" robot of the family [52,61]. Since the equation coefficients are continuous functions of the geometric parameters, a continuous path

Table 3 DGP of the 3-3 CDPR presented in Table 2: real potential solutions

Geometric dimensions and load: $\mathbf{a}_2 = [10; 0; 0], \mathbf{a}_3 = [0; 12; 0], \mathbf{b}'_1 = [1; 0; 0], \mathbf{b}'_2 = [0; 1; 0], \mathbf{b}'_3 = [0; 0; 1], (\rho_1, \rho_2, \rho_3) = (7.5, 10, 9.5), Q = 10.$

Conf.	$(e_1, e_2, e_3; x, y, z)$	(τ_1, τ_2, τ_3)	$\mathbf{H}_r$	Fig. 2
1	(−4.2220216376218525374, −5.9041632869515210360, −0.47192841642603461020; +1.6804603696020390943, +3.5743047536049493407, +5.5605475750988856764)	(+6.84, +3.05, +6.14)	<>	(2*a*)
2	(−3.3553981637732204646, +0.5425359168641715099, +1.7110227662077546889; +2.9313331749199504570, +4.0768903590846968732, +6.0451905744644536057)	(+5.26, +5.11, +5.81)	>	(2*b*)
3	(−2.6616890629909497781, +0.4160373487571940226, +0.9655548628886102991; +2.5977352480361477511, +3.8457865212868645040, −4.8661048045758031135)	(−5.71, −4.85, −5.59)	<>	
4	(−2.5291311336353393166, +7.3670838551717188775, −3.0436947470784328872; +4.3757198849572551337, +5.8522722689950264632, −4.0010370837572794347)	(−1.40, −9.30, −9.83)	>	
5	(−1.1658499286472699650, −1.2731250301592223731, −1.0066002786209496830; +1.3992607683511133116, +3.2794852510182088478, +5.5312834538826469464)	(+6.76, +2.51, +4.86)	<>	(2*c*)
6	(−0.5483498696623835987, −0.4877188327940637588, −1.2105960172659885404; (+1.8159313811036966479, +4.3022189513770458215, +5.5516371755216273886)	(+5.46, +3.25, +5.50)	<>	(2*d*)
7	(−0.5044737581189470443, +2.5903097146888037712, −1.2479550929596409397; +3.5231344366003843222, +5.5320236367500482920, +5.2626779413057278297)	(+2.89, +7.87, +9.12)	<>	(2*e*)
8	(−0.3252555841337169146, −0.8891989606461705137, −1.6130562813850683595; +2.5760653793782856615, +4.3924466541541392403, −6.7527508537785241857)	(−4.61, −4.12, −5.65)	<	
9	(+0.5434332197723969320, −0.1455056574282349313, +0.5696219999523911064; +3.0240954483208687602, +4.7309738515237873056, +3.3019215367593690362)	(+5.90, +7.83, +9.56)	<	(2*f*)
10	(+0.6844447542486557310, −0.0996112288836193264, +0.5262976928395059876; +2.8401864910572365897, +4.8133317875987522652, −4.4534720523569757781)	(−6.01, −7.61, −9.53)	<>	
...	...	...	...	

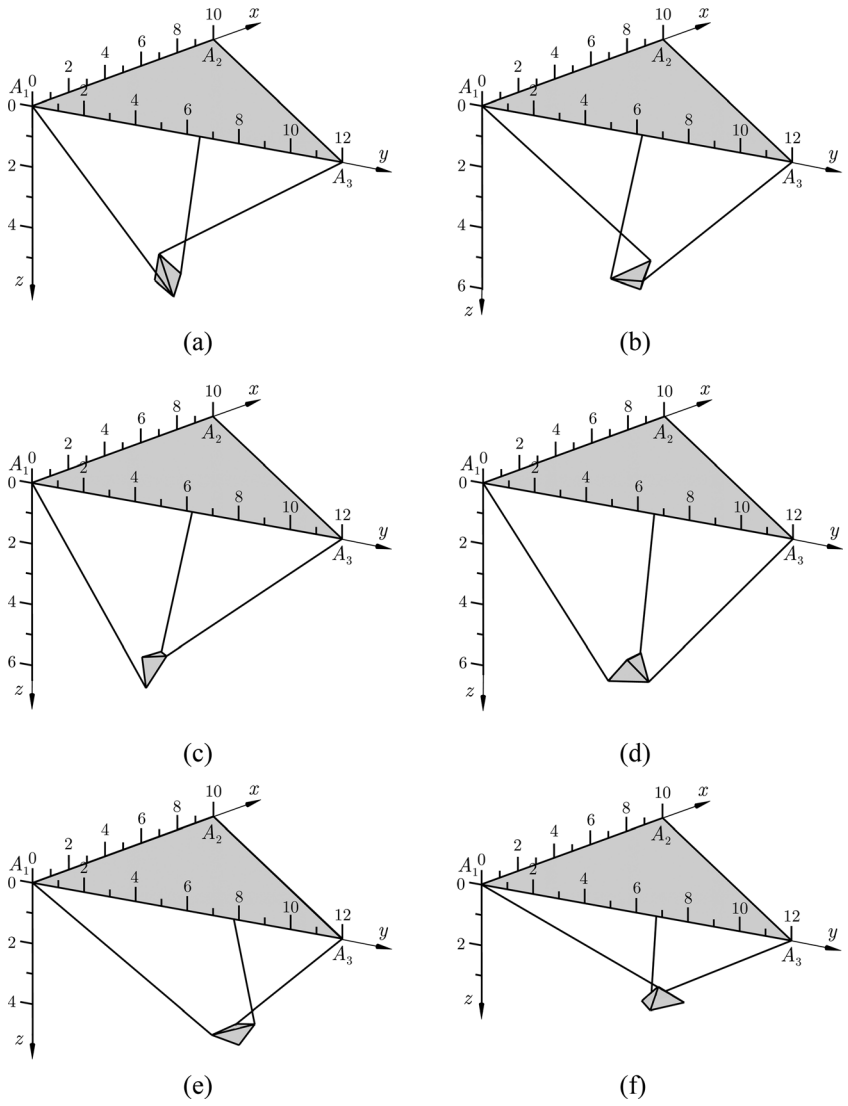

Fig. 2 DGP of the 3-3 CDPR presented in Table 2: equilibrium configurations with nonnegative tension in all cables

through parameter space determines a continuous evolution of the coefficients and, generally, continuous paths for the solutions as well. Accordingly, by a suitable homotopy [62], only the paths originating at the isolated roots of the start system (in a number equal to 156) may be tracked, whereas those corresponding to solutions at infinity (which cause unbeneficial computational burden) may be ignored. By using parameter continuation and default settings, BERTINI computes the finite solutions to J_{red}, for the robot whose geometric parameters are reported in Table 2, in roughly 6.2 min.

A more efficient implementation of the parameter-continuation routine may be constructed on the basis of the system S formed by the geometric constraints in Eq. (3) and the static relations in Eq. (4), which include cable tensions among the unknowns. S contains nine scalar relations in nine variables (i.e., $\mathbf{X}$ and $\boldsymbol{\tau}$) and it has a much larger Bezout number compared to J_{red}, namely, 4800 against 1920. Nonetheless, this does not result in a larger number of paths to be followed when parameter continuation is performed, since only the 156 paths corresponding to the finite solutions of the start system are tracked. Furthermore, S comprises simpler lower-order polynomials compared to J_{red}, and this produces paths that may be tracked in a considerably more rapid and stabler way. By this implementation, BERTINI is able to compute the finite solutions to S in less than 1.4 min, for the robot in Table 2.

As for the eigenvalue formulations presented in Sec. 3.3.1, the solution search cannot be limited to predefined domains, so that it is not possible to incorporate constraints on the unknowns in the continuation routine. It is necessary to calculate all roots of Eqs. (3) and (4) (real and complex, regardless of the sign of cable tensions), and then use a postprocessing step to eliminate inadmissible solutions. For a more detailed discussion about the application of continuation methods to the DGP of the 3-3 CDPR, the reader may refer to Ref. [62].

3.3.3 Interval Analysis. Another approach to efficiently solve the DGP of the 3-3 in practical cases relies on techniques based on interval analysis. The latter have the following interesting properties [63]:

- real-value geometric parameters may be directly handled in floating-point arithmetic;
- results are guaranteed against numerical computer round-off errors;
- real solutions may be directly searched for, and constraints on the unknowns (particularly lower and upper bounds on cable tensions) may be easily incorporated within the problem-solving routine;
- the abundance of linearly independent equations available in J allows lower computation times to be attained, by enriching

Table 4 DGP of a 3-3 CDPR with 54 real potential solutions

Geometric dimensions and load: $\mathbf{a}_2 = [0.87239; 0; 0.087941]$, $\mathbf{a}_3 = [0.31752; 0.48646; -0.016501]$, $\mathbf{b}'_1 = [-0.78466; -0.35058; 0.48115]$, $\mathbf{b}'_2 = [0.46664; -0.35058; 0.48115]$, $\mathbf{b}'_3 = [-0.00704; 0.47275; 0.48115]$, $(\rho_1, \rho_2, \rho_3) = (1, 0.95110, 0.73758)$, $Q = 10$.

Conf.	$(e_1, e_2, e_3; x, y, z)$	(τ_1, τ_2, τ_3)	$\mathbf{H}_r$
1	(−5.4614294311925020053, +0.0173536807147813177, −0.3100210753440456029); (+0.3935472842368857842, +0.1808111691242998204, +1.0383599167105029146)	(+4.26, +4.05, +7.42)	>
2	(−4.1797214292900880282, −6.8478347950258985815, +0.3514991521292444341); (+0.7103362119654336397, +0.0958262602998788014, +0.7810086923081841400)	(+4.98, +14.34, +9.51)	>
3	(−2.3841200362918340257, −2.3394159764963221491, +0.8490321441619597505); (+0.8607788314718697152, −0.0037527353690492382, +0.7552546007023042315)	(+0.36, +13.79, +10.83)	<>
4	(−0.4863019644307176738, −2.1657311861304995048, −0.2863725216731426209); (+0.9686378130633803271, +0.0868818876119070610, +0.7354857781799160742)	(+7.21, +13.16, +3.10)	<>
5	(−0.2013943322393901434, −0.0453416376226155101, +0.0515296024454830576); (+0.5283918784779030256, +0.0792999430885494435, +0.4244176372233764265)	(+3.02, +5.55, +1.70)	>
6	(+1.4255092412518180719, −2.6189943609918970012, +0.3505962651985286990); (+0.5085291895448221065, +0.3290333889906895434, +0.9262916536766926699)	(+7.02, +4.41, +7.77)	>
7	(+3.5322905636419180394, +5.8388951790075283681, −0.0970283274196336667); (+0.4060218349169291586, +0.2419089653712617907, +0.7766016270169904300)	(+6.20, +14.29, +11.45)	>
8	(+4.5169587479064276016, +7.4484757910582396270, −0.1526687793821966507); (+0.4428326095347329080, +0.2245389964586149584, +0.7765833645732042240)	(+6.27, +14.89, +11.63)	<>
...	...	...	...

the set of available tests that may be used to exclude portions of the search domain from the solution search;

- uncertainties in the parameter values, e.g., due to manufacturing tolerances or measuring errors, may be easily taken into account.

A drawback of interval analysis is that efficiency is heavily dependent upon the choice of heuristics implemented in the problem-solving algorithm. For a given problem, computation time may vary from seconds to hours, depending on the specific heuristics that are used.

Preliminary results concerning the application of interval analysis to the DGP of the 3-3 CDPR may be found in Ref. [64]. Results are promising, as the feasible solutions to the DGP of a generic robot may be ordinarily found in less than 2 min, and there is room for significant further improvements.

3.4 Number of Real-Valued Solutions. The 156 solutions computed by the methods presented in Sec. 3.3 may be complex or real, but only the latter have physical interest. By varying the robot parameters in $\mathbb{R}^{21}$, the count of real roots changes. However, since there may be roots in the solution set that always remain complex, the maximal number of real solutions may be smaller than 156. Determining a tight bound for this count is a challenging task.

Three numerical approaches were developed in Ref. [62], namely, a continuation procedure adapted from an algorithm originally proposed by Dietmaier [65] to determine the maximum number of real assembly modes of the Stewart-Gough platform and two evolutionary procedures. In the first approach, an arbitrary set of the parameters defining the manipulator geometry is chosen, and all real and complex solutions of the corresponding DGP are computed. Successively, the robot parameters are modified in such a way that the imaginary parts of pairs of complex conjugate roots are caused to vanish and new pairs of real roots are brought into existence. By the iterative application of the procedure, the number of real solutions is maximized. The evolutionary procedures are based, respectively, on a genetic algorithm and particle swarm optimization. In both cases, maximizing the number of real equilibrium poses is set as the objective function.

By all methods, several sets of robot parameters for which the DGP provides at the most 54 real configurations were found. The coherence of the obtained results may lead to conjecture that the achieved bound is tight, even though formal proof is yet to be discovered. Table 4 reports one of the aforementioned sets. Due to space limitations, only the real solutions with nonnegative tension in all cables are reported. Even though the geometric dimensions of the robot are not particularly meaningful under a practical point of view, the example shows that the DGP of the 3-3 CDPR may admit *multiple* feasible configurations: in this case, in fact, 5 out of 54 real equilibrium configurations have positive tension in all cables and are stable, thus being feasible.

4 Equilibrium Configurations With Unloaded Cables

When cable lengths are assigned as inputs, nothing ensures, a priori, that when the platform reaches its stable equilibrium pose all cables are under tension. Accordingly, the final pose may be *either* a DGP solution for the current 3-3 CDPR *or* a valid pose for any one of the *m–m* CDPRs (with $m < 3$) that may be derived from the initial 3-3 robot. Accordingly, the overall solution set must be obtained by solving the DGP for *all* possible constraint sets $\{||\mathbf{s}_j|| = \rho_j, j \in \mathcal{W}\}$, with $\mathcal{W} \subseteq \{1, 2, 3\}$ and $\text{card}(\mathcal{W}) \leq 3$, and by retaining, for each corresponding solution set, only the solutions for which $||\mathbf{s}_k|| < \rho_k, k \notin \mathcal{W}$. In general, this amounts to solving 7 DGPs, namely, 1 DGP with 3 cables in tension, 3 DGPs with 2 cables in tension and 3 DGPs with 1 cable in tension. The solution of the problem with a single taut cable is trivial, whereas the complete solution of the DGP of a CDPR suspended by 2 cables is available in Ref. [37].

When the DGP admits multiple feasible solutions, and these are "sufficiently" close to each other, the robot may switch (because of inertia forces or external disturbances) across portions of the configuration space characterized by different numbers of taut cables, thus bringing the end-effector onto unpredicted trajectories. Accordingly, the computation of the complete set of equilibrium configurations is essential for robust trajectory planning. This motivates and gives relevance to the algorithms presented in this paper.

5 Conclusions

This paper studied the kinematics and statics of underconstrained CDPRs with 3 cables, in crane configuration. For such robots, kinematics and statics are coupled and they must be dealt with simultaneously. This poses major challenges, since displacement analysis problems gain remarkable complexity with respect to those of analogous six-dofs rigid-link robots.

An original geometrico-static model was presented, which allowed the DGP to be effectively worked out and the complete solution set to be determined. The DGP aims at determining the platform pose and the cable tensions once the cable lengths are assigned. A least-degree univariate polynomial in the ideal governing the problem was obtained by an innovative hybrid procedure relying on Groebner bases, the FGLM algorithm and Dhingra et al. dialytic elimination, thus showing that 156 solutions exist in the complex field. The procedure encompassed three steps. First, a Grobner basis G was calculated with respect to an efficient monomial order (such as grevlex). Then, a subset of the original unknowns was eliminated by computing, by way of the FGLM algorithm, a Groebner basis G_l of a suitable elimination ideal. Finally, a least-degree univariate polynomial devoid of extraneous factors was computed by applying dialytic elimination to the polynomials of G_l. The adopted approach appeared to provide a profitable technique to compute a least-degree univariate polynomial in a polynomial ideal. By considerably reducing computation requirements, in terms of both memory and time, it was successful when other methods either failed or proved to be excessively onerous in terms of computational burden.

The 156 solutions of the DGP were numerically computed via three alternative approaches, namely

- an eigenproblem associated with the Groebner-basis computation,
- homotopy continuation,
- interval analysis.

The advantages and drawbacks of each approach were critically discussed.

The problem of identifying a robot geometry providing the highest number of *real* equilibrium configurations was addressed. Based on a study presented in Ref. [62], the maximal number of real-valued solutions of the DGP was conjectured to be equal to 54. However, the big gap between the maximal number of complex and real solutions still deserves in-depth investigation.

Equilibrium configurations with slack cables were finally discussed.

All reported solution counts concern potential solutions of the problems at hand, since they do not take into account the constraints imposed by the sign of cable tensions and the stability of equilibrium. Once such constraints are imposed and solutions are sifted, the number of *feasible* configurations is drastically reduced. When multiple feasible configurations exist, the end-effector may switch across them, due to inertia forces or external disturbances. Computing the complete set of equilibrium configurations is, thus, essential for a robust trajectory planning.

The problem-solving methods presented in this paper have general validity and they may be profitably used to solve the DGP of CDPRs suspended by more than 3 cables or characterized by special geometries (these typically emerge when some cable anchor points on the base and/or the platform coalesce). Clearly, in all these cases, the maximal number of solutions is likely to change. Preliminary results about generic CDPRs with 4 and 5 cables may be found in Refs. [42,43], respectively.

Acknowledgment

The author wishes to express his gratitude to Dr. J.-P. Merlet. Even though Dr. Merlet could not co-author this paper, his advice and guidance were essential for the achievements therein reported. The author gratefully acknowledges the financial support of the 2007-2013 ERDF Emilia-Romagna Regional Operational Programme at the Interdepartmental Center for Health Sciences and Technologies.

References

[1] Roberts, R. G., Graham, T., and Lippitt, T., 1998, "On the Inverse Kinematics, Statics, and Fault Tolerance of Cable-Suspended Robots," J. Rob. Syst., **15**(10), pp. 581–597.
[2] Kawamura, S., Kino, H., and Won, C., 2000, "High-Speed Manipulation by Using Parallel Wire-Driven Robots," Robotica, **18**(1), pp. 13–21.
[3] Tadokoro, S., Murao, Y., Hiller, M., Murata, R., Kohkawa, H., and Matsushima, T., 2002, "A Motion Base With 6-DOF by Parallel Cable Drive Architecture," IEEE/ASME Trans. Mechatron., **7**(2), pp. 115–123.
[4] Hiller, M., Fang, S., Mielczarek, S., Verhoeven, R., and Franitza, D., 2005, "Design, Analysis And Realization of Tendon-Based Parallel Manipulators," Mech. Mach. Theory, **40**(4), pp. 429–445.
[5] Alikhani, A., Behzadipour, S., Vanini, S. A. S., and Alasty, A., 2009, "Workspace Analysis of a Three DOF Cable-Driven Mechanism," ASME J. Mech. Rob., **1**(4), p. 041005.
[6] Landsberger, S. E., 1984, "Design and Construction of a Cable-Controlled, Parallel Link Manipulator," Master's thesis, Massachusetts Institute of Technology, Department of Mechanical Engineering, Cambridge.
[7] Behzadipour, S., and Khajepour, A., 2005, "A New Cable-Based Parallel Robot With Three Degrees of Freedom," Multibody Syst. Dyn., **13**(4), pp. 371–383.
[8] Albus, J., Bostelman, R., and Dagalakis, N., 1993, "The NIST Robocrane," J. Rob. Syst., **10**(5), pp. 709–724.
[9] Su, Y. X., Duan, B. Y., Nan, R. D., and Peng, B., 2001, "Development of a Large Parallel-Cable Manipulator for the Feed-Supporting System of a Next-Generation Large Radio Telescope," J. Rob. Syst., **18**(11), pp. 633–643.
[10] Bosscher, P., Riechel, A. T., and Ebert-Uphoff, I., 2006, "Wrench-Feasible Workspace Generation for Cable-Driven Robots," IEEE Trans. Rob., **22**(5), pp. 890–902.
[11] Stump, E., and Kumar, V., 2006, "Workspaces of Cable-Actuated Parallel Manipulators," ASME J. Mech. Des., **128**(1), pp. 159–167.
[12] Ghasemi, A., Eghtesad, M., and Farid, M., 2009, "Workspace Analysis for Planar and Spatial Redundant Cable Robots," ASME J. Mech. Rob., **1**(4), p. 044502.
[13] Diao, X., and Ma, O., 2009, "Force-Closure Analysis of 6-DOF Cable Manipulators With Seven or More Cables," Robotica, **27**(2), pp. 209–215.
[14] Bouchard, S., Gosselin, C., and Moore, B., 2010, "On the Ability of a Cable-Driven Robot to Generate a Prescribed Set of Wrenches," ASME J. Mech. Rob., **2**(1), p. 011010.
[15] Gouttefarde, M., Daney, D., and Merlet, J.-P., 2011, "Interval-Analysis-Based Determination of the Wrench-Feasible Workspace of Parallel Cable-Driven Robots," IEEE Trans. Rob., **27**(1), pp. 1–13.
[16] Lau, D., Oetomo, D., and Halgamuge, S., 2011, "Wrench-Closure Workspace Generation for Cable Driven Parallel Manipulators Using a Hybrid Analytical-Numerical Approach," ASME J. Mech. Des., **133**(7), p. 071004.
[17] Azizian, K., and Cardou, P., 2012, "The Dimensional Synthesis of Planar Parallel Cable-Driven Mechanisms Through Convex Relaxations," ASME J. Mech. Rob., **4**(3), p. 031011.
[18] Behzadipour, S., and Khajepour, A., 2006, "Stiffness of Cable-Based Parallel Manipulators With Application to Stability Analysis," ASME J. Mech. Des., **128**(1), pp. 303–310.
[19] Surdilovic, D., Radojicic, J., and Krüger, J., 2013, "Geometric Stiffness Analysis of Wire Robots: A Mechanical Approach," *Cable-Driven Parallel Robots*, T. Bruckmann and A. Pott, eds., Springer-Verlag, Berlin Heidelberg, pp. 389–404.
[20] Merlet, J.-P., 2004, "Analysis of the Influence of Wires Interference on the Workspace of Wire Robots," *On Advances in Robot Kinematics*, J. Lenarčič and C. Galletti, eds., Kluwer Academic Publishers, Dordrecht, pp. 211–218.
[21] Perreault, S., Cardou, P., Gosselin, C. M., and Otis, M. J.-D., 2010, "Geometric Determination of the Interference-Free Constant-Orientation Workspace of Parallel Cable-Driven Mechanisms," ASME J. Mech. Rob., **2**(3), p. 031016.
[22] Pusey, J., Fattah, A., Agrawal, S., and Messina, E., 2004, "Design and Workspace Analysis of a 6-6 Cable-Suspended Parallel Robot," Mech. Mach. Theory, **39**(7), pp. 761–778.
[23] Rosati, G., Zanotto, D., and Agrawal, S. K., 2011, "On the Design of Adaptive Cable-Driven Systems," ASME J. Mech. Rob., **3**(2), p. 021004.
[24] Yamamoto, M., Yanai, N., and Mohri, A., 2004, "Trajectory Control of Incompletely Restrained Parallel-Wire-Suspended Mechanism Based on Inverse Dynamics," IEEE Trans. Rob., **20**(5), pp. 840–850.
[25] Fattah, A., and Agrawal, S. K., 2006, "On the Design of Cable-Suspended Planar Parallel Robots," ASME J. Mech. Des., **127**(5), pp. 1021–1028.
[26] Heyden, T., and Woernle, C., 2006, "Dynamics and Flatness-Based Control of a Kinematically Undetermined Cable Suspension Manipulator," Multibody Syst. Dyn., **16**(2), pp. 155–177.
[27] Michael, N., Kim, S., Fink, J., and Kumar, V., 2009, "Kinematics and Statics of Cooperative Multi-Robot Aerial Manipulation With Cables," ASME 2009 International Design Engineering Technical Conferences, San Diego, Vol. 7, pp. 83–91, Paper No. DETC2009–87677.
[28] Jiang, Q., and Kumar, V., 2010, "The Inverse Kinematics of 3-D Towing," *Advances in Robot Kinematics: Motion in Man and Machine*, J. Lenarčič and M. M. Stanišič, eds., Springer, Dordrecht, pp. 321–328.
[29] Jiang, Q., and Kumar, V., 2010, "The Direct Kinematics of Objects Suspended From Cables," ASME 2010 International Design Engineering Technical Conferences, Montreal, Canada, Vol. 2, pp. 193–202, Paper No. DETC2010–28036.
[30] Collard, J.-F., and Cardou, P., 2013, "Computing the Lowest Equilibrium Pose of a Cable-Suspended Rigid Body," Optim. Eng., (in press).
[31] Morizono, T., Kurahashi, K., and Kawamura, S., 1998, "Analysis and Control of a Force Display System Driven by Parallel Wire Mechanism," Robotica, **16**(5), pp. 551–563.
[32] Surdilovic, D., Zhang, J., and Bernhardt, R., 2007, "STRING-MAN: Wire-Robot Technology for Safe, Flexible and Human-Friendly Gait Rehabilitation," Proceedings of the 2007 IEEE International Conference on Rehabilitation Robotics, Noordwijk, The Netherlands, pp. 446–453.
[33] Rosati, G., Gallina, P., and Masiero, S., 2007, "Design, Implementation and Clinical Tests of a Wire-Based Robot for Neurorehabilitation," IEEE Trans. Neural Syst. Rehabil. Eng., **15**(4), pp. 560–569.

[34] Merlet, J.-P., and Daney, D., 2010, "A Portable, Modular Parallel Wire Crane for Rescue Operations," Proceedings of the 2010 IEEE International Conference on Robotics and Automation, Anchorage, pp. 2834–2839.
[35] Gobbi, M., Mastinu, G., and Previati, G., 2011, "A Method for Measuring the Inertia Properties of Rigid Bodies," Mech. Syst. Signal Process., **25**(1), pp. 305–318.
[36] Carricato, M., and Merlet, J.-P., 2010, "Geometrico-Static Analysis of Under-Constrained Cable-Driven Parallel Robots," *Advances in Robot Kinematics: Motion in Man and Machine*, J. Lenarčič and M. M. Stanišič, eds., Springer, Dordrecht, pp. 309–319.
[37] Carricato, M., and Merlet, J.-P., 2013, "Stability Analysis of Underconstrained Cable-Driven Parallel Robots," IEEE Trans. Rob., **29**(1), pp. 288–296.
[38] Merlet, J.-P., 2013, "Wire-Driven Parallel Robot: Open Issues," *Romansy 19 – Robot Design, Dynamics and Control*, V. Padois, P. Bidaud, and O. Khatib, eds., Springer, Vienna, pp. 3–10.
[39] McCarthy, J. M., 2011, "21st Century Kinematics: Synthesis, Compliance, and Tensegrity," ASME J. Mech. Rob., **3**(2), p. 020201.
[40] Carricato, M., 2013, "Inverse Geometrico-Static Problem of Under-Constrained Cable-Driven Parallel Robots With Three Cables," ASME J. Mech. Rob., **5**(4), p. 041002.
[41] Carricato, M., Abbasnejad, G., and Walter, D., 2012, "Inverse Geometrico-Static Analysis of Under-Constrained Cable-Driven Parallel Robots With Four Cables," *Latest Advances in Robot Kinematics*, J. Lenarčič and M. Husty, eds., Springer, Dordrecht, pp. 365–372.
[42] Carricato, M., and Abbasnejad, G., 2013, "Direct Geometrico-Static Analysis of Under-Constrained Cable-Driven Parallel Robots With 4 Cables," *Cable-Driven Parallel Robots*, T. Bruckmann and A. Pott, eds., Springer-Verlag, Berlin Heidelberg, pp. 269–285.
[43] Abbasnejad, G., and Carricato, M., 2013, "Direct Geometrico-Static Problem of Underconstrained Cable-Driven Parallel Robots With 5 Cables," Proceedings of the 6th International Workshop on Computational Kinematics, Barcelona, Spain.
[44] Raghavan, M., and Roth, B., 1995, "Solving Polynomial Systems for the Kinematic Analysis and Synthesis of Mechanisms and Robot Manipulators," ASME J. Mech. Des., **117**(2B), pp. 71–79.
[45] Carricato, M., and Merlet, J.-P., 2011, "Direct Geometrico-Static Problem of Under-Constrained Cable-Driven Parallel Robots With Three Cables," 2011 IEEE International Conference on Robotics and Automation, Shanghai, China, pp. 3011–3017.
[46] Bottema, O., and Roth, B., 1990, *Theoretical Kinematics*, Dover Publications, New York.
[47] Morgan, A., and Sommese, A., 1987, "A Homotopy for Solving General Polynomial Systems That Respects m-Homogeneous Structures," Appl. Math. Comput., **24**(2), pp. 101–113.
[48] Morgan, A., and Sommese, A., 1987, "Computing all Solutions to Polynomial Systems Using Homotopy Continuation," Appl. Math. Comput., **24**(2), pp. 115–138.
[49] Wampler, C. W., 1992, "Bezout Number Calculations for Multi-Homogeneous Polynomial Systems," Appl. Math. Comput., **51**(2–3), pp. 143–157.
[50] Merlet, J.-P., 2006. *Parallel Robots*, Springer, Dordrecht.
[51] Dhingra, A. K., Almadi, A. N., and Kohli, D., 2000, "A Gröbner-Sylvester Hybrid Method for Closed-Form Displacement Analysis of Mechanisms," ASME J. Mech. Des., **122**(4), pp. 431–438.
[52] Sommese, A. J., and Wampler, C. W., 2005, *The Numerical Solution of Systems of Polynomials Arising in Engineering and Science*, World Scientific Publishing, Singapore.
[53] Cox, D., Little, J., and O'Shea, D., 2007, *Ideals, Varieties, and Algorithms*, Springer, New York.
[54] Faugère, J. C., Gianni, P., Lazard, D., and Mora, T., 1993, "Efficient Computation of Zero-Ddimensional Gröbner Bases by Change of Ordering," J. Symb. Comput., **16**(4), pp. 329–344.
[55] Möller, H. M., 1998, "Gröbner Bases and Numerical Analysis," *Gröbner Bases and Applications*, Vol. 251 of London Mathematical Society Lecture Note Series, B. Buchberger and F. Winkler, eds., Cambridge University Press, Cambridge, pp. 159–178.
[56] Corless, R. M., 1996, "Gröbner Bases and Matrix Eigenproblems," ACM SIGSAM Bull., **30**(4), pp. 26–32.
[57] Manocha, D., and Krishnan, S., 1996, "Solving Algebraic Systems Using Matrix Computations," ACM SIGSAM Bull., **30**(4), pp. 4–21.
[58] Higham, N., Mackey, D., and Tisseur, F., 2006, "The Conditioning of Linearizations of Matrix Polynomials," SIAM J. Matrix Anal. Appl., **28**(4), pp. 1005–1028.
[59] Higham, N., Li, R.-C., and Tisseur, F., 2007, "Backward Error of Polynomial Eigenproblems Solved by Linearization," SIAM J. Matrix Anal. Appl., **29**(4), pp. 1218–1241.
[60] Bates, D. J., Hauenstein, J. D., Sommese, A. J., and Wampler, C. W., "BERTINI: Software for Numerical Algebraic Geometry," Available at: http://bertini.nd.edu
[61] Morgan, A. P., and Sommese, A. J., 1989, "Coefficient-Parameter Polynomial Continuation," Appl. Math. Comput., **29**(2), pp. 123–160.
[62] Abbasnejad, G., and Carricato, M., 2012, "Real Solutions of the Direct Geometrico-Static Problem of Under-Constrained Cable-Driven Parallel Robots With 3 Cables: A Numerical Investigation," Meccanica, **47**(7), pp. 1761–1773.
[63] Merlet, J.-P., 2009, "Interval Analysis for Certified Numerical Solution of Problems in Robotics," Int. J. Appl. Math. Comput. Sci., **19**(3), pp. 399–412.
[64] Berti, A., Merlet, J.-P., and Carricato, M., 2013, "Solving the Direct Geometrico-Static Problem of 3-3 Cable-Driven Parallel Robots by Interval Analysis: Preliminary Results," *Cable-Driven Parallel Robots*, T. Bruckmann and A. Pott, eds., Springer-Verlag, Berlin Heidelberg, pp. 251–268.
[65] Dietmaier, P., 1998, "The Stewart-Gough Platform of General Geometry can have 40 Real Postures," *Advances in Robot Kinematics: Analysis and Control*, J. Lenarčič and M. L. Husty, eds., Kluwer Academic Publishers, Dordrecht, pp. 7–16.